Static and dynamic properties of 0, π, and 0-π ferromagnetic Josephson tunnel junctions

J. Pfeiffer,* M. Kemmler, D. Koelle, R. Kleiner, and E. Goldobin
Physikalisches Institut-Experimentalphysik II and Center for Collective Quantum Phenomena, Universität Tübingen, D-72076 Tübingen, Germany

M. Weides
Center of Nanoelectronic Systems for Information Technology (CNI), Research Center Jülich, D-52425 Jülich, Germany

A. K. Feofanov, J. Lisenfeld, and A. V. Ustinov
Physikalisches Institut III, Universität Erlangen-Nürnberg, D-91058 Erlangen, Germany

(Received 18 January 2008; revised manuscript received 23 April 2008; published 10 June 2008)

We present experimental studies of static and dynamic properties of 0, π, and 0-π superconductor-insulator-ferromagnet-superconductor (SIFS) Josephson junctions of small and intermediate length. In the underdamped limit, these junctions exhibit a rich dynamical behavior such as resonant steps on the current-voltage characteristics. Varying the experimental conditions, zero-field steps, Fiske steps, and Shapiro steps are observed with a high resolution. A strong signature of the 0-π Josephson junction is demonstrated by measuring the critical current as a function of two components (B_x and B_y) of an in-plane magnetic field. The experimental observation of a *half-integer zero-field step* in 0-π SIFS junctions is presented.

DOI: 10.1103/PhysRevB.77.214506 PACS number(s): 74.50.+r, 74.78.Fk, 74.25.Ha, 85.25.Cp

I. INTRODUCTION

The interplay between superconductivity and ferromagnetism has been studied during many decades,[1] but only during the last few years considerable results have been achieved regarding the experimental realization of π and 0-π Josephson junctions (JJs) using superconductor-ferromagnet multilayers. In such structures, the Cooper pair wave function penetrates into the ferromagnet in the form of damped oscillations.[2,3] If the thickness d_F of the ferromagnetic barrier is of the order of half the oscillation period, the superconducting wave function changes its sign, i.e., shifts its phase by π while crossing the ferromagnet. In superconductor-ferromagnet-superconductor (SFS) or superconductor-insulator-ferromagnet-superconductor (SIFS) JJs this leads to a negative critical current I_c and the current-phase relation reads $I=I_c \sin(\phi)=|I_c|\sin(\phi+\pi)$ with $I_c<0$. Such a JJ is called "π JJ" because it has $\phi=\pi$ in the ground state, i.e., when no bias current is applied. In this context, conventional JJs are called "0 JJ" because they have a current-phase relation of $I=I_c \sin\phi$ with $I_c>0$ and the ground-state phase $\phi=0$. In experiment, a single 0 JJ and a single π JJ are indistinguishable, as one can only determine $|I_c|$ because on current-voltage characteristics we have both $\pm I_c$, so that the sign of I_c is invisible. During the last years several experiments showed a change in the sign of I_c as a function of temperature[4] T or of the thickness of the ferromagnetic barrier[5–8] d_F. The signatures of π JJs were also demonstrated by embedding SFS JJs into superconducting loops.[9–11] π JJs are supposed to improve the performance of various classical and quantum electronic circuits, e.g., they can be used in rapid single flux quantum (RSFQ) logics to self-bias the circuit and to reduce the number of bias resistors[12] and inductances[13] or to design environmentally decoupled "quiet" flux qubits.[14,15] Depending on the target parameters, SFS or SIFS JJs are used. An advantage of SIFS JJs is that their resistance-area product $R\times A$ can be tuned over orders of magnitude by varying the thickness d_I of the insulating barrier. A high $R\times A$ product facilitates voltage readout and allows us to observe dynamic behavior of the junction due to low damping. Thus, these junctions can be used not only as phase batteries but also as active switching elements in superconducting electronic circuits. By contrast, SFS JJs have a small $R\times A$ product and are always in the overdamped limit.

An intentionally made symmetric 0-π SIFS JJ with two reference junctions was demonstrated recently.[16] Before that, 0-π JJs were realized by utilizing d-wave superconductors[17–20] or were obtained by chance using SFS technology.[21,22] These SFS 0-π JJs had a very small $R\times A$ product, an accidentally achieved 0-π phase boundary, and no reference junctions were available. The 0-π SIFS JJ of Ref. 16 consisted of 0 and π parts with equal critical current densities, as can be concluded from the measurements of the reference junctions. This 0-π JJ had a high characteristic voltage $V_c=I_cR$ making direct transport measurements possible. The JJs could be driven into the underdamped regime by decreasing the temperature below 4.2 K. Tuning the temperature, the same absolute critical current densities in both parts were achieved. In this symmetric case, the ground state of the system consists of a spontaneously formed vortex of supercurrent circulating around the 0-π boundary. This supercurrent corresponds to a local magnetic flux $|\Phi|\leq\Phi_0/2$, where $\Phi_0=h/2e$ is the magnetic-flux quantum. In the case of a very long 0-π JJ, the flux $\Phi=\pm\Phi_0/2$, and thus the localized magnetic field, is called *semifluxon*.[23] A 0-π SIFS JJ is a promising system to study the physics of semifluxons. One can also use 0-π-0 SIFS JJs to design semifluxon molecule qubits.[24,25] No restrictions in topology, low damping, and good reproducibility make the 0, π and 0-π JJs good candidates for future logic elements.

In this paper, we study dynamic and static properties of 0-π SIFS JJs and of the corresponding reference 0 and π JJs. The junction parameters allow us to investigate the over-

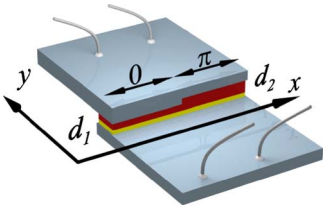

FIG. 1. (Color online) Sketch of a SIFS 0-π Josephson junction with a steplike change in the thickness d_F (from d_1 to d_2) of the F-layer along the x axis. Top and bottom electrodes are shown by light blue (gray) color, the insulating barrier is yellow (light gray), and the ferromagnetic barrier is red (dark gray).

damped as well as the underdamped regime by varying the temperature between 310 mK and 4.2 K. Various resonant steps on the current-voltage characteristics are observed. Special attention is paid to the signatures of the 0-π boundary.

II. EXPERIMENTAL RESULTS

A. Samples

Our SIFS Josephson junctions are fabricated in overlap geometry using Nb/Al-Al_2O_3/$Ni_{60}Cu_{40}$/Nb technology.[26,27] Varying the thickness d_F of the ferromagnetic barrier, Josephson junctions with 0 and π ground states are obtained.[8] To fabricate 0-π SIFS Josephson junctions, the ferromagnetic layer was selectively etched along one-half of the junction. In this way one-half of the junction has a F-layer thickness $d_F=d_1$ and, if taken separately, would be in a ground state with a phase drop of zero, while the other half of the junction has a F-layer thickness $d_F=d_2$ and, if taken separately, would be in a ground state with a phase drop of π.[16] A schematic drawing of such a 0-π long JJ is shown in Fig. 1. The lengths of the 0 and π parts are equal with a lithographic accuracy of less than 1 μm. For each 0-π JJ two reference junctions (one 0 JJ with $d_F=d_1$ and one π JJ with $d_F=d_2$), having the same length L as the 0-π JJ, are fabricated in the same run. We assume that the critical current density j_c^0 is the same in the 0 JJ and in the 0 part of the 0-π JJ. Similarly, j_c^π is the same in the π JJ and in the π part of the 0-π JJ.

In this paper, we present experimental data for two sets of samples. Each set is situated on a separate chip (chip 1 and chip 2) and contains three JJs: a 0-π JJ, a 0 JJ, and a π JJ. The thickness d_I of the insulating barrier is smaller on chip 2 than on chip 1, resulting in higher critical current densities in comparison with chip 1. The junction parameters are summarized in Table I. The critical current densities of the reference junctions are obtained by measuring their I-V characteristics (IVCs), while for the 0-π JJs, only the average value $j_c^{0\text{-}\pi}=(|j_c^\pi|+j_c^0)/2$ is quoted. $j_c^{0\text{-}\pi}$ is used to calculate the normalized lengths l of the 0-π JJs. Actually, this $j_c^{0\text{-}\pi}$ value is a simplified picture to facilitate the calculations. It is different from the measured critical current density in a 0-π JJ, i.e., from $j_c^{0\text{-}\pi}$ at $B=0$, a situation when the critical currents in both halves are partially or totally canceling each other. While calculating l the idle region corrections are taken into account.[28,29] Note that early measurements using sample set 1 were already published.[16] The measurements reported here were done at least eight months later. It turned out that some parameters, e.g., j_c values, slightly changed with time presumable due to the clustering in the F layer and degradation of the interfaces.

The measurements are carried out in a standard ^{4}He or ^{3}He cryostat. The ^{4}He cryostat can be evacuated so that temperatures from 4.2 K down to 2.1 K are reachable. Using the ^{3}He cryostat, temperatures between 1.9 and 310 mK are accessible. In both measurement setups, different mu-metal or cryoperm shields are placed around the sample to shield it from the earth magnetic field or stray fields. Each sample could be prepared in a flux-free state by a cycling procedure, i.e., the sample was warmed above the critical temperature and cooled down again.

B. Static properties

We study the static properties of sample set 1 by measuring the dependences of the critical current on magnetic field $I_c(B)$. The junctions are cooled down in the absence of externally applied magnetic field or bias current to provide a flux-free state. Magnetic fields with both x and y components can be applied in the plane of the junctions (see Fig. 1). The $I_c^0(B_x,B_y)$ and $I_c^\pi(B_x,B_y)$ dependences of the 0 and π reference junctions have almost perfect Fraunhofer patterns (not shown), indicating a state without trapped flux. The maxima of the curves reveal a small offset from zero magnetic field probably due to a weak net magnetization of the ferromag-

TABLE I. Parameters of the investigated samples at measurement temperatures. L is the length of the junction, $W_{j,i}$ is the width of the junction or the idle region in physical units. l is the normalized length of the respective JJ. Notations are chosen according to Ref. 29.

id @ T (K)	j_c (A/cm^2)	l	L (μm)	W_j (μm)	W_i (μm)
1-0 @ 4.2	2.1	0.72	330	30	50
1-π @ 4.2	1.5	0.62	330	30	50
1-0-π @ 4.2	1.8	0.67	330	30	50
2-0 @ 0.34	13.4	3.1	500	12.5	10
2-π @ 0.34	4.5	1.8	500	12.5	10
2-0-π @ 0.34	9.0	2.5	500	12.5	10

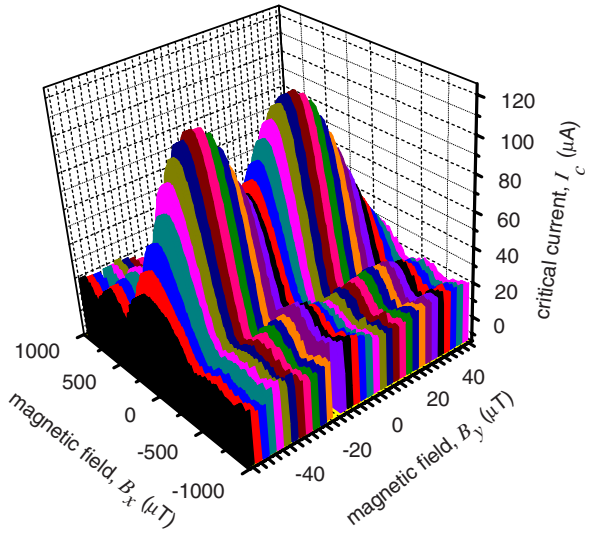

FIG. 2. (Color online) Experimentally measured $I_c^{0\text{-}\pi}(B_x,B_y)$ of sample 1-0-π at T=4.2 K. For B_y=0, $I_c^{0\text{-}\pi}(B_x)$ shows a regular Fraunhofer pattern. For B_x=0, in $I_c^{0\text{-}\pi}(B_y)$, a minimum around $B_y \sim 0$ is visible which is a characteristic feature of 0-π JJs.

net. Applying only B_x, the field value at the first minimum of $I_c(B_x)$ dependence is ~11 times larger than the corresponding value on the $I_c(B_y)$ curve. This corresponds to the ratio between the length L and the width W_j of the Josephson junctions on chip 1 (L/W_j=11/1).

Figure 2 shows the $I_c^{0\text{-}\pi}(B_x,B_y)$ dependence of the 0-π junction of set 1. Applying a magnetic field in the x direction results in an almost perfect Fraunhofer pattern, indicating that no parasitic flux is trapped in the junction or its electrodes. Applying magnetic field in the y direction a well pronounced minimum around zero field is visible. This minimum is a characteristic feature of a 0-π Josephson junction.[18,30,31] Thus, Fig. 2 leaves no doubts that the observed behavior is due to the step in the ferromagnetic barrier and not due to some other reasons. The normalized junction length is calculated as l=0.67 at T=4.2 K. In contrast to earlier investigations of this sample,[16] the idle region corrections[28,29] are now taken into account. Although the junction is short in terms of λ_J ($l<1$), I_c in the central minimum on the $I_c^{0\text{-}\pi}(B_y)$ dependence does not reach zero as it should be for a short JJ,[32] most probably because $j_c^0 \neq j_c^\pi$ at T=4.2 K. The asymmetry factor is estimated as $\Delta=j_c^\pi/j_c^0$ =0.71, i.e., the critical current densities in the 0 and π parts differ by about 30%. For such an asymmetry the ground state is fluxless.[33]

C. Dynamic properties

We study the dynamic properties by measuring IVCs. The IVCs directly reveals the relationship between the average flux velocity v, which is proportional to the measured dc voltage V, and the driving force, which is proportional to the bias current I. To observe dynamics, the junction under examination has to be in the underdamped regime. This is typically the case for temperatures below ~3 K. At T=4.2 K, none of our samples is underdamped. By decreasing the temperature, all junctions become underdamped.

1. Half-integer zero-field steps in 0-π junctions

If IVC measurements are carried out *in the absence of magnetic field* or microwaves, one can observe so-called zero-field steps (ZFSs) on the IVC of a JJ. They have a voltage position given by

$$V_n^{ZFS} = \frac{\Delta\Phi}{\Delta t} = n\frac{2\Phi_0\bar{c}}{2L} = n\frac{\Phi_0\bar{c}}{L}. \quad (1)$$

where $\bar{c}$ is the Swihart velocity. Thus, the voltage spacing between the ZFSs is $\Delta V^{ZFS}=\Phi_0\bar{c}/L$.

Fiske steps (FSs) appear on the IVCs of JJs in magnetic field when the parameter $l/\sqrt{\beta_c}$ is relatively small. Physically, a Fiske resonance is the synchronization between a moving Josephson vortex chain and a standing electromagnetic wave in the JJ. The resonance number n determines the number of wavelengths of the standing wave. The asymptotic voltage of the nth Fiske step is given by

$$V_n^{FS} = n\frac{\Phi_0\bar{c}}{2L}, \quad (2)$$

i.e., the voltage spacing between Fiske steps is twice smaller than for ZFSs.

These expectations are met in our experiments in the underdamped limit with the 0 and π junction of sample set 1. The observed ZFSs have a voltage spacing which is exactly two times larger than the one of Fiske steps (not shown). In the case of the 0-π junction, the first ZFS emerges at exactly *half* of the usual ZFS spacing, i.e., exactly at *the same* voltage as the first Fiske step, according to the earlier predictions[34,35] and to experiments on 0-π JJs of other types.[32] Figure 3(a) shows IVCs of the JJ 1-0-π measured at different T and at B=0. At 35 μV, which is exactly the observed value of the Fiske step voltage spacing in this sample, a step is emerging for $T<3.8$ K. The step appears due to the flipping of a fractional vortex.[32] At zero-bias current, for our JJ length and j_c asymmetry, the ground state of the system is a flat phase state ϕ=0 (fluxless). As soon as a uniform bias current is applied, a fractional flux (Josephson vortex) localized at the 0-π boundary and carrying a bias current dependent flux appears.[36] Since the junction has a finite length, the interaction of this vortex with the boundary can be treated as the interaction of the vortex with an antivortex (image) situated outside the junction at the same distance from the edge. There are two such images, one behind the left and one behind the right edge of the JJ [see the inset of Fig. 3(a)]. The bias current exerts a Lorenz force which tries to collide the vortex with one of the images. If the bias is large enough, both the vortex and the image vortex flip, changing polarity and exchanging one flux quantum, which, in fact, is passing through the JJ boundary. Then a similar process takes place between the fractional vortex (now of negative polarity) and another image, so one Φ_0 passes through the other JJ boundary. Assuming that the maximum velocity of flux transfer is $\bar{c}$, we calculate that the asymptotic voltage is exactly equal to the voltage of the first Fiske step.

In order to show that the observed step is indeed a ZFS, the maximum current $I_m^{0\text{-}\pi}$ of this step versus magnetic field B_y is measured, see Fig. 3(b). The $I_m^{0\text{-}\pi}(B_y)$ has a maximum in

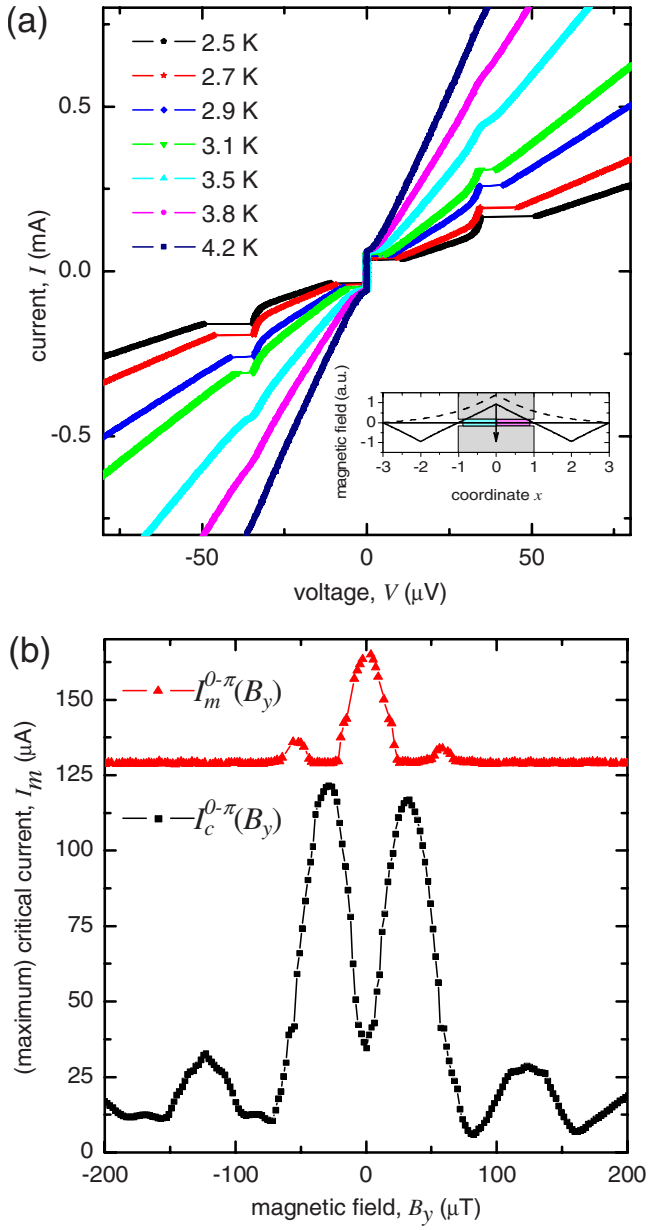

FIG. 3. (Color online) (a) Experimentally measured IVCs of JJ 1-0-π at different temperatures. At $T<3.8$ K, the half-integer zero-field step is emerging. The inset shows the sketch of a 0-π JJ with a fractional vortex which is permanently flipping. (b) The dependence of the maximum current $I_m^{0\text{-}\pi}$ of the first half-integer ZFS at $V=35$ μV on magnetic field B_y, measured at $T=2.5$ K. The $I_c^{0\text{-}\pi}(B_y)$ dependence is shown for comparison.

zero field and is decreasing with applied magnetic field—which is the typical behavior of a ZFS. The background value of $I_m^{0\text{-}\pi}$ corresponds to the current on the McCumber branch at $V\approx 35$ μV below which the step cannot be suppressed in principle. Figure 3(b) additionally shows the $I_c^{0\text{-}\pi}(B_y)$ curve measured at the same temperature of $T=2.5$ K for comparison. The minimum around $B_y\approx 0$, typical for 0-π JJs is visible. Note that the amplitude of $I_c(B_y)$ is higher than in Fig. 2 as the temperature is lower. The next ZFS emerges at ~ 100 μV ($n=3/2$) and corresponds to one additional fluxon moving inside the 0-π JJ. Comparable measurements are performed for sample set 2 and show similar results (not shown). Up to now, half-integer ZFS have been observed only in artificial 0-π junctions.[32] To our knowledge, here we report on the first measurements of a half-integer ZFS in 0-π SIFS junctions.

2. Fiske steps

By applying a magnetic field B_y to sample set 2, various Fiske steps were observed on the IVCs. The data presented below are taken at $T=340$ mK (underdamped regime) for sample 2-π.

The low-voltage part of several IVCs of junction 2-π at different magnetic fields in the range $-105\cdots 105$ μT is shown in Fig. 4(a). Nine Fiske steps are observed with a high resolution. Similar Fiske step measurements were also carried out for samples 2-0-π and 2-0 (not shown). To summarize these measurements, in Fig. 4(b) we plot the voltage positions of Fiske steps versus step number for all three samples. The first four Fiske steps have an almost equidistant voltage spacing. For higher Fiske steps, the voltage spacing between adjacent Fiske steps shrinks with increasing step number. Thus, the dispersion relation of electromagnetic waves in the junctions is not linear. A possible explanation might be the layout of the junctions and the fabrication process: inhomogeneities in the junction may result in a decreasing voltage spacing of resonant steps on the IVC, compare with Ref. 37. Local inhomogeneities are, e.g., nonideal junction boundaries, where the profile of the critical current does not sharply go to zero but is smeared out. This is the case if the junction is surrounded by a large idle region, which is true for our samples.

As visible in Fig. 4(b), the Fiske step voltage spacing of the π junction shows the smallest deviation from an equidistant voltage spacing, indicating a better homogeneity as compared to the 0 and 0-π junctions. Note that the F layer of the last two junctions (or parts of it) is etched during the fabrication process. The etching might cause additional inhomogeneities. This topic was already discussed in the literature as *material dispersion*.[38,39] The authors had shown that due to idle region effects or a frequency dependent magnetic penetration depth, summarized as material dispersion, the dispersion relation of electromagnetic waves in JJs is not linear.

Another explanation is that j_c^0 is more sensitive to variations in d_F (roughness) than j_c^π because d_1 and d_2 are chosen so that

$$\left|\frac{\partial I_c(d_F)}{\partial d_F}\right|_{d_F=d_1} > \left|\frac{\partial I_c(d_F)}{\partial d_F}\right|_{d_F=d_2}, \tag{3}$$

see Fig. 1 of Ref. 8.

To calculate the capacitance of the junctions the voltage spacing of the first four Fiske steps is used. The capacitance is estimated as $C\approx 22.9\pm 0.8$ μF/cm^2 which also includes idle region effects. From geometrical considerations, the contributions of the idle region (C_i) and the *naked* junction (C_j) to the capacitance $C=C_i+C_j$ can be estimated. The respective capacitance is calculated as $C_{i,j}=\epsilon_0\epsilon_{i,j}W_{i,j}L/d_I^{i,j}$, L being the length and $W_{i,j}$ being the width of the junction or idle region (see Table I).

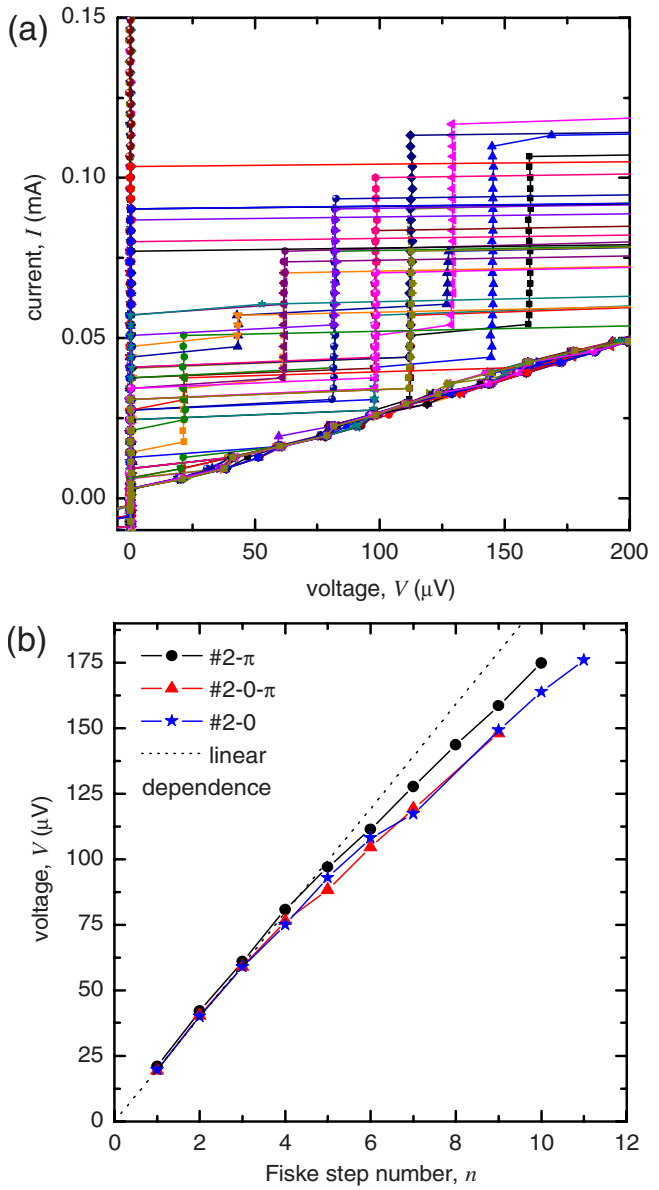

FIG. 4. (Color online) (a) Fiske steps on the IVCs of junction 2-π at $T=340$ mK. The magnetic field is varied between $B=-105$ and 105 μT. (b) Asymptotic voltage of the nth Fiske step is plotted versus n for sample set 2. Taking into account only the first four Fiske steps $\Delta V=19.9$ μV.

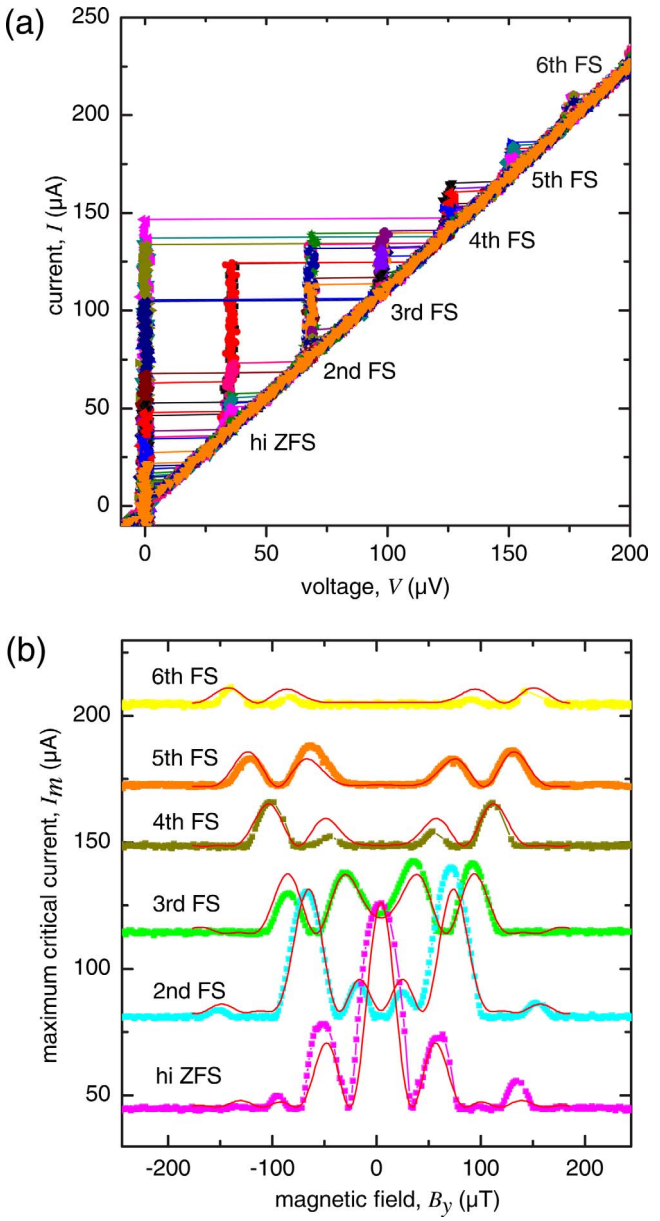

FIG. 5. (Color online) (a) Experimental data of Fiske steps on the IVCs of junction 1-0-π at $T=310$ mK. The magnetic field is varied between $B=-200$ and 200 μT. hi=half-integer. (b) Maximum current amplitude of the nth Fiske step versus applied magnetic field at $T=310$ mK. Solid line: analytical calculations performed according to Ref. 40 using the experimental parameters of sample 1-0-π at $T=310$ mK.

Taking $\epsilon_i \sim 30$ and $\epsilon_j \sim 10$ and $d_I^i=120$ nm and $d_I^j=0.4$ nm, the idle region has a capacitance of $C_i=221.5$ nF/cm^2. The Swihart velocity in the naked junction is calculated as $c_0=c\sqrt{d_I^j/\epsilon_j d_j'}$, with c being the vacuum speed of light and $\mu_0 d_j'$ being the inductance (per square) of the junction electrodes, resulting in $c_0=0.015c$.

Comparable Fiske step measurements are performed for sample set 1. The low-voltage part of several IVCs of sample 1-0-π at $T=310$ mK is shown in Fig. 5(a). The magnetic field is varied between $B=-200$ and 200 μT. In Fig. 5(b) the dependences of the maximum current of the Fiske steps on magnetic field are presented. Note that every odd FS is mixed with a half-integer ZFS, thus resulting in a finite step height even for $B=0$. Our experimental data reproduce theoretical predictions rather well.[40] Nappi *et al.*[40] used a perturbative scheme to calculate phase dynamics and the resulting resonances appearing on the IVC of JJs with an arbitrary number of 0-π singularities. As realized in our samples, they considered the flat phase regime where no spontaneous flux is occurring in the ground state of a JJ with finite length. Using expressions (27) and (28) from Ref. 40 with the respective parameters of our samples we are able to compare experiment and theory, see solid lines in Fig. 5(b). The analytical calculations are performed in normalized units and converted to physical units by a fitting procedure: The x axis

is adjusted by superimposing the first minimum of the $I_m^{0\text{-}\pi}(B_y)$ curve of the half-integer ZFS in experiment and theory. This conversion scheme is used for all six measurements. The y axes are adjusted separately using a similar procedure. We find a very good agreement between the analytical predictions and the experimental data. The spacing of the minima, the height of the maxima, and the overall shape of the curves are reproduced by theory.[40]

As it was pointed out, each odd step is a mixture of Fiske and half-integer ZFS. The amplitude $I_m(0)$ of the third step is above the background level due to its ZFS contribution. For the fifth FS, $I_m(0)$ coincides with the background level as the ZFS contribution is vanishing.

3. Shapiro steps

Shapiro step measurements are carried out for sample set 1. IVCs are measured at different temperatures in the presence of applied microwaves. Constant voltage steps appear on the IVC due to the synchronization of Josephson oscillations to the applied excitation. As an example, Shapiro step measurements for sample 1-0 at $T=4.2$ K and $T=3.2$ K are shown in Fig. 6. Microwave frequencies of $f=2$ GHz and $f=4$ GHz are applied. In both cases, resonant steps, which fulfill the condition, $\Delta V=f\Phi_0$ (4.1 μV and 8.3 μV, respectively) are observed. Additionally, half-integer Shapiro steps are visible which have a voltage spacing of $\Delta V=\frac{1}{2}(f\Phi_0)$. They are weakly pronounced for $f=2$ GHz at $T=4.2$ K [see inset of Fig. 6(a)]. At $T=4.2$ K, the junction is in the overdamped regime. These experimental conditions are chosen to avoid chaotic dynamics. With decreasing temperature and increasing frequency the half-integer Shapiro steps become more pronounced [see Fig. 6(b)].

The occurrence of half-integer Shapiro steps reminds one of the ongoing discussion about nonsinusoidal current-phase relations in 0-π junctions. As already described, a 0 to π transition can be achieved in SFS or SIFS junctions as a function of temperature[4] or ferromagnetic barrier thickness.[6] As close to the 0-π transition, the first-order Josephson supercurrent vanishes; the observation of a $\sin(2\phi)$ component seems possible in the transition region. Half-integer Shapiro steps have been reported for SFS junctions in the vicinity of the minimum of I_c.[41] The authors attributed these steps to the $\sin(2\phi)$ component. In other experiments,[22] half-integer Shapiro steps are explained with a nonuniform critical current density, without the need of an intrinsic $\sin(2\phi)$ component. Thus, the conclusive explanation of the origin of half-integer Shapiro steps is still an open problem.

In order to examine whether our half-integer Shapiro steps are due to a nonsinusoidal current-phase relation, Shapiro step measurements for different excitation amplitudes are carried out. As an example, the experimental parameters I_c and R of sample 1-0 at $T=4.2$ K are obtained from experiment and are used for simulations. Current-voltage characteristics can be simulated according to the resistively and capacitively shunted junction (RCSJ) model (see inset of Fig. 7) A current-phase relation is used with an additional $\sin(2\phi)$ term, which can be weighted by a factor of δ. Shapiro steps are measured in experiment by radiating microwaves with a frequency $f=2$ GHz. As a first try simulations are performed

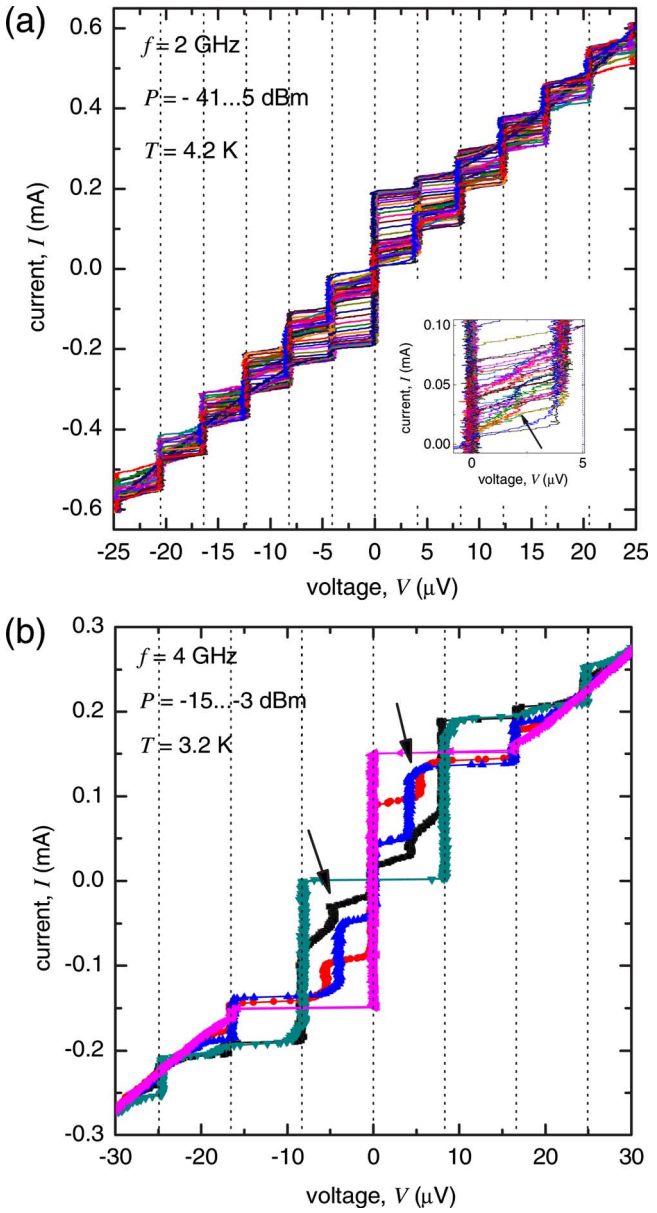

FIG. 6. (Color online) (a) Shapiro steps measured for junction 1-0 at $T=4.2$ K (overdamped regime). Microwaves are applied with a frequency of $f=2$ GHz; the power is varied between $P=-41$ and 5 dBm. Voltage spacing between the Shapiro steps is calculated as $\Delta V=4.1$ μV (dotted lines). Inset: enlargement of the $0\cdots5$ μV region shows a weak half-integer Shapiro step. (b) Experimental data of Shapiro step measurements of the same junction at $T=3.2$ K (underdamped regime). As $f=4$ GHz, a voltage spacing of $\Delta V=8.3$ μV (dotted lines) is expected. Half-integer Shapiro steps are visible and marked by the arrows.

without taking the $\sin(2\phi)$ component into account ($\delta=0$). The height of the Shapiro steps is extracted from experimental data and from simulations. As expected the respective step heights are proportional to the Bessel functions. In Fig. 7 we compare the height of the Shapiro steps with $n=0,1,\frac{1}{2}$ as a function of applied microwave power, obtained in experiment and simulation. One can see a perfect quantitative agreement. Although the $\sin(2\phi)$ component is not taken into account, the half-integer Shapiro step appears in

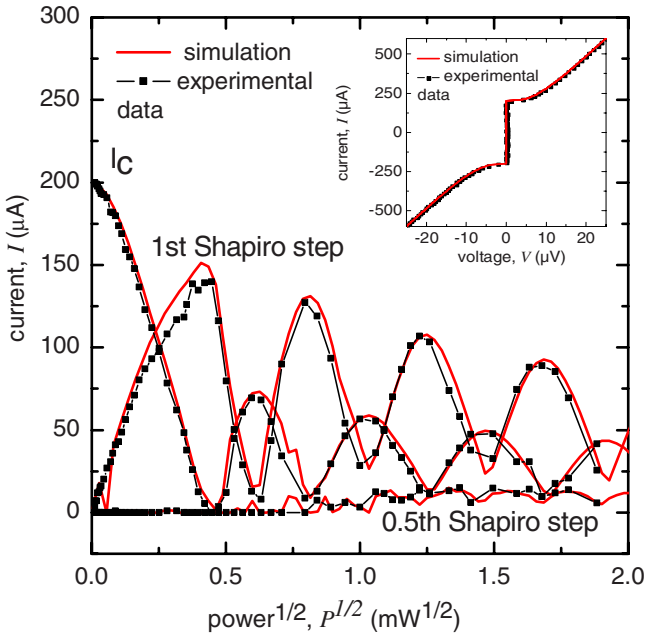

FIG. 7. (Color online) Dependence of the height of the zeroth ($=I_c$), first, and 0.5th Shapiro steps on the applied microwave power. Experimental data and simulations are compared. Simulations are performed without taking the $\sin(2\phi)$ component into account. Inset: comparison between experimentally observed IVC and according to the RCSJ-model simulated curve (sample: 1-0 at $T=4.2$ K, $f=2$ GHz, $I_c=202.8$ μA, and $\beta_c=0.8$).

the simulations and reproduces the experimental data perfectly well. This is a result of a finite capacitance, i.e., $\beta_c \neq 0$.

The simulations are repeated taking the $\sin(2\phi)$ component into account (not shown). As long as the second harmonic is small ($\delta \leq 0.1$), the experimental data are reproduced by the numerical simulations. As soon as the second-harmonic contribution is higher than $\delta > 0.1$, the simulations deviate significantly from the experimental data. These data confirm our assumption that the half-integer Shapiro steps are not due to a $\sin(2\phi)$ contribution. Half-integer Shapiro steps are also observed for samples 1-π and 1-0-π (not shown). The experimental data are reproduced in simulations without the need of a $\sin(2\phi)$ component, too. Nevertheless, half-integer Shapiro steps are observed here in systems in which the $\sin(2\phi)$ component does not play a dominant role as the $\sin\phi$ component is not suppressed. In this case, the half-integer Shapiro step is a subharmonic step and not attributed to a double Josephson frequency.

III. CONCLUSIONS

We experimentally studied the static and *dynamic* properties of 0, π, and 0-π SIFS Josephson junctions using two sets of samples: 1 being in the short junction limit and 2 having an intermediate junction length. All samples can be made underdamped at sufficiently low temperatures below $T=4.2$ K. Fiske steps, zero-field steps, and Shapiro steps were observed on the *I-V* characteristics. The dynamic properties of 0 and π SIFS junctions are qualitatively similar to standard superconductor-insulator-superconductor junctions.

We have observed half-integer Shapiro steps on the current-voltage characteristics of 0, π, and 0-π Josephson junctions, which does not necessarily imply the presence of the second harmonic in the current-phase relation but may be present due to the finite capacitance of the Josephson junctions. The analysis of a short overdamped JJ in the framework of the RSJ model confirms this picture.

Half-integer zero-field steps were observed on the *I-V* characteristics of 0-π Josephson junctions. The $I_m^{0\text{-}\pi}(B_y)$ dependences for several Fiske and zero-field steps were measured. Before half-integer zero-field steps were observed only in "artificial" 0-π JJs.[32] Thus, SIFS 0, π, and 0-π JJ technology can already be used to fabricate more complex superconducting electronic devices combining the dynamics of fluxons and semifluxons, e.g., using RSFQ readout for semifluxon bits and/or qubits or ballistic fluxon readout.[42,43]

ACKNOWLEDGMENTS

We thank T. Gaber for useful discussions. Financial support by the Studienstiftung des Deutschen Volkes (J.P.), by the Evangelisches Studienwerk e.V. Villigst (M.K.), by the DFG (Projects No. WE 4359/1-1, No. SFB/TRR 21, and No. GO 1106/1-1), and by INTAS (Grant No. 05-1000008-7972) is gratefully acknowledged.

*judith.pfeiffer@uni-tuebingen.de

[1] A. I. Buzdin, Rev. Mod. Phys. **77**, 935 (2005).
[2] P. Fulde and R. A. Ferrell, Phys. Rev. **135**, A550 (1964).
[3] A. Larkin and Y. N. Ovchinnikov, Sov. Phys. JETP **20**, 762 (1965).
[4] V. V. Ryazanov, V. A. Oboznov, A. Y. Rusanov, A. V. Veretennikov, A. A. Golubov, and J. Aarts, Phys. Rev. Lett. **86**, 2427 (2001).
[5] Y. Blum, A. Tsukernik, M. Karpovski, and A. Palevski, Phys. Rev. Lett. **89**, 187004 (2002).
[6] T. Kontos, M. Aprili, J. Lesueur, F. Genêt, B. Stephanidis, and R. Boursier, Phys. Rev. Lett. **89**, 137007 (2002).
[7] V. A. Oboznov, V. V. Bol'ginov, A. K. Feofanov, V. V. Ryazanov, and A. I. Buzdin, Phys. Rev. Lett. **96**, 197003 (2006).
[8] M. Weides, M. Kemmler, E. Goldobin, D. Koelle, R. Kleiner, H. Kohlstedt, and A. Buzdin, Appl. Phys. Lett. **89**, 122511 (2006).
[9] V. V. Ryazanov, V. A. Oboznov, A. V. Veretennikov, and A. Y. Rusanov, Phys. Rev. B **65**, 020501(R) (2001).
[10] W. Guichard, M. Aprili, O. Bourgeois, T. Kontos, J. Lesueur, and P. Gandit, Phys. Rev. Lett. **90**, 167001 (2003).
[11] A. Bauer, J. Bentner, M. Aprili, M. L. Della-Rocca, M. Reinwald, W. Wegscheider, and C. Strunk, Phys. Rev. Lett. **92**, 217001 (2004).
[12] T. Ortlepp, Ariando, O. Mielke, C. J. M. Verwijs, K. F. K. Foo,

H. Rogalla, F. H. Uhlmann, and H. Hilgenkamp, Science **312**, 1495 (2006).
[13] A. V. Ustinov and V. K. Kaplunenko, J. Appl. Phys. **94**, 5405 (2003).
[14] L. B. Ioffe, V. B. Geshkenbein, M. V. Feigel'man, A. L. Faucheère, and G. Blatter, Nature (London) **398**, 679 (1999).
[15] T. Yamashita, K. Tanikawa, S. Takahashi, and S. Maekawa, Phys. Rev. Lett. **95**, 097001 (2005).
[16] M. Weides, M. Kemmler, E. Goldobin, H. Kohlstedt, R. Waser, D. Koelle, and R. Kleiner, Phys. Rev. Lett. **97**, 247001 (2006).
[17] C. C. Tsuei and J. R. Kirtley, Rev. Mod. Phys. **72**, 969 (2000).
[18] H.-J. H. Smilde, Ariando, D. H. A. Blank, G. J. Gerritsma, H. Hilgenkamp, and H. Rogalla, Phys. Rev. Lett. **88**, 057004 (2002).
[19] D. J. Van Harlingen, Rev. Mod. Phys. **67**, 515 (1995).
[20] H. Hilgenkamp, Ariando, H.-J. H. Smilde, D. H. A. Blank, G. Rijnders, H. Rogalla, J. R. Kirtley, and C. C. Tsuei, Nature (London) **422**, 50 (2003).
[21] M. L. Della Rocca, M. Aprili, T. Kontos, A. Gomez, and P. Spathis, Phys. Rev. Lett. **94**, 197003 (2005).
[22] S. M. Frolov, D. J. Van Harlingen, V. V. Bolginov, V. A. Oboznov, and V. V. Ryazanov, Phys. Rev. B **74**, 020503(R) (2006).
[23] E. Goldobin, D. Koelle, and R. Kleiner, Phys. Rev. B **66**, 100508(R) (2002).
[24] T. Kato and M. Imada, J. Phys. Soc. Jpn. **66**, 1445 (1997).
[25] E. Goldobin, K. Vogel, O. Crasser, R. Walser, W. P. Schleich, D. Koelle, and R. Kleiner, Phys. Rev. B **72**, 054527 (2005).
[26] M. Weides, C. Schindler, and H. Kohlstedt, J. Appl. Phys. **101**, 063902 (2007).
[27] M. Weides, K. Tillmann, and H. Kohlstedt, Physica C **437-438**, 349 (2006).
[28] A. Wallraff, Ph.D. thesis, University of Erlangen, 2001; http://fluxon.physik.uni-erlangen.de
[29] R. Monaco, G. Costabile, and N. Martucciello, J. Appl. Phys. **77**, 2073 (1995).
[30] D. A. Wollman, D. J. Van Harlingen, W. C. Lee, D. M. Ginsberg, and A. J. Leggett, Phys. Rev. Lett. **71**, 2134 (1993).
[31] J. R. Kirtley, K. A. Moler, and D. J. Scalapino, Phys. Rev. B **56**, 886 (1997).
[32] E. Goldobin, A. Sterck, T. Gaber, D. Koelle, and R. Kleiner, Phys. Rev. Lett. **92**, 057005 (2004).
[33] L. N. Bulaevskii, V. V. Kuzii, and A. A. Sobyanin, Solid State Commun. **25**, 1053 (1978).
[34] N. Stefanakis, Phys. Rev. B **66**, 214524 (2002).
[35] N. Lazarides, Phys. Rev. B **69**, 212501 (2004).
[36] E. Goldobin, D. Koelle, and R. Kleiner, Phys. Rev. B **67**, 224515 (2003).
[37] P. Barbara, R. Monaco, and A. V. Ustinov, J. Appl. Phys. **79**, 327 (1996).
[38] Z. Hermon, A. Stern, and E. Ben-Jacob, Phys. Rev. B **49**, 9757 (1994).
[39] G. S. Lee and A. T. Barfknecht, IEEE Trans. Appl. Supercond. **2**, 67 (1992).
[40] C. Nappi, E. Sarnelli, M. Adamo, and M. A. Navacerrada, Phys. Rev. B **74**, 144504 (2006).
[41] H. Sellier, C. Baraduc, F. Lefloch, and R. Calemczuk, Phys. Rev. Lett. **92**, 257005 (2004).
[42] E. Goldobin, N. Stefanakis, D. Koelle, and R. Kleiner, Phys. Rev. B **70**, 094520 (2004).
[43] A. Herr (Kidiyarova-Shevchenko), A. Fedorov, A. Shnirman, E. Ilichev, and G. Schoen, Supercond. Sci. Technol. **20**, S450 (2007).